J. Synchrotron Rad. (1999). **6**, 758–760

Why does Ni suppress superconductivity in $La_{1.85}Sr_{0.15}Cu_{1-y}Ni_yO_4$?

Daniel Haskel,[a]* Edward A. Stern,[a] Victor Polinger[a] and Fatih Dogan[b]

[a]Department of Physics, University of Washington, Seattle WA 98195 USA, and [b]Department of Materials Science and Engineering, University of Washington, Seattle WA 98195 USA. E-mail: haskel@phys.washington.edu

The role played by Ni impurities in destroying the superconducting state of $La_{2-x}Sr_xCuO_4$ is still unclear. This is partly due to the lack of clear experimental evidence on the effect of Ni substitution upon the atomic and electronic structure of this cuprate. To provide this information, we performed Ni K-edge polarized XAFS measurements on oriented powder. A special magnetic alignment geometry allowed us to measure pure $\hat{c}$ and $\widehat{ab}$-polarized XAFS in identical experimental conditions.

We found that the NiO_6 octahedra are contracted along the $\hat{c}$-axis by 0.16(Å) relative to the CuO_6 octahedra in $La_{1.85}Sr_{0.15}CuO_4$, dragging La atoms and causing the observed macroscopic $\hat{c}$-axis contraction. This contraction reflects the non-Jahn-Teller $3d^8$ state of Ni in this compound (similar to that in La_2NiO_4) and indicates that Ni does not "trap" hole carriers but rather, probably, "repels" them. We suggest that this repulsion is the mechanism behind T_c suppression.

Keywords: superconductivity, nickel doping, Jahn-Teller.

1. Introduction

The importance of *local* effects around dopant atoms to the mechanism of T_c suppression by Ni and Zn impurities in $La_{2-x}Sr_xCuO_4$ has been recently stressed by several groups. Local variations of the superconducting order parameter have been theoretically predicted to occur within very short distances (order of few Fermi wavelengths k_F^{-1}) from impurity sites (Zhitomirsky & Walker, 1998). A "swiss cheese" model was suggested based on muon spin relaxation (μSR) measurements, in which hole carriers within an area $\pi\zeta_{ab}^2$ around each impurity (ζ_{ab} the in-plane superconducting coherence length) are excluded from the superfluid, lowering the condensate density and limiting the formation of a macroscopically coherent Bose-condensed superconducting state (Nachumi *et. al*, 1996). A different interpretation of nearly identical μSR data by Bernhard *et. al* claims that the observed reduction in superfluid density with doping is well explained in terms of a d-wave order parameter and pair breaking arising from scattering at the dopant sites (Bernhard *et. al*, 1996; Bernhard *et. al*, 1998).

These *local* effects are particularly important in the high T_c cuprates, as their very short planar coherence length ($\zeta_{ab} \approx 20 - 30$ Å)(Suzuki & Hikita, 1989; Nachumi *et. al*, 1996) is comparable to the average distance between dopant atoms in the CuO_2 plane for a few at. % dopant concentration y, i.e., $r_i = (3.77\, y^{-1/2})$[Å]. It is clear that a complete understanding of the role of local effects requires knowledge of the local atomic environment around the dopant atoms. Diffraction cannot provide such information as it measures the average of the Cu/Ni environments, dominated by the Cu majority sites. XAFS is element specific, so it can determine the Ni environment separately. In addition, polarization dependence is crucial for obtaining information on the O(2) apical oxygens to Ni, as the first shell O signal in a powder XAFS experiment is dominated by the much larger in-plane O(1) signal (the planar Ni-O(1) bonds are highly covalent and rigid compared to the softer Ni-O(2) bonds; also the planar coordination number is twice as large).

2. Experimental

$La_{1.85}Sr_{0.15}Cu_{1-y}Ni_yO_4$ powders with y=0.01, 0.03, 0.06 were synthesized from nitrates. Sintering of powder compacts ($\approx$ 3 grams) took place at 1140°C for 24 hrs. Lattice parameters were refined at room temperature using 14 reflections of the $I4/mmm$ space group; zero field cooled T_c's were measured by SQUID magnetometry in a H=1 G applied field. Results of both measurements are shown in figure 1.

Polarized XAFS measurements were taken on magnetically aligned powder ($\hat{c}$-axis aligned, random in $\widehat{ab}$ plane) in fluorescence (Ni K-edge) and transmission (La, Sr K-edges) at beamline X-11A of the National Synchrotron Light Source using Si(111) (Ni, Sr) and Si(311) (La) double crystal monochromators. A special magnetic alignment procedure was implemented for the Ni experiment allowing measuring *pure* $\hat{c}$-polarized data in the same experimental conditions as for the $\widehat{ab}$ one (i.e., incident x-ray beam at 45°, see figure 2). A $\sim 30\mu$m aluminum foil was used to minimize fluorescence background dominated by La $L_{\alpha,\beta}$ lines. Ni K-edge XAFS is limited to ≈ 13 Å^{-1} due to the appearance of Cu K-edge in the absorption spectra.

3. Analysis and Results

Data is analyzed with the UWXAFS package (Stern *et. al*, 1995) together with theoretical standards from FEFF6 (Zabinsky *et. al*, 1995). Polarization dependence of the XAFS signal is included in the theoretical calculations, where the appropiate angular averaging is performed for $\hat{c}$-aligned powder but randomly oriented in the $\widehat{ab}$ plane. Data with $\hat{E} \parallel \hat{c}$, $\hat{E} \perp \hat{c}$ are refined simultaneously, significantly reducing the number of fitting parameters relative to the number of independent points in the data for paths that contribute in both orientations. Coordination numbers are set to their average structure values in the undoped structure (Radaelli *et. al*, 1994).

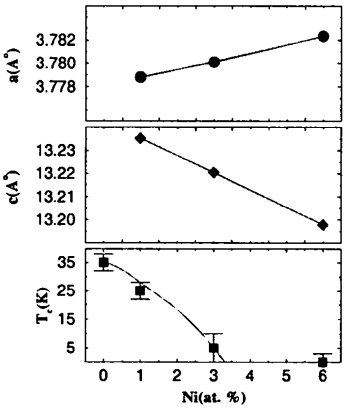

Figure 1
Lattice parameters and T_c's for Ni doped $La_{1.85}Sr_{0.15}CuO_4$ at RT. The value of T_c for $y = 0$ is from Radaelli *et. al*, 1994.

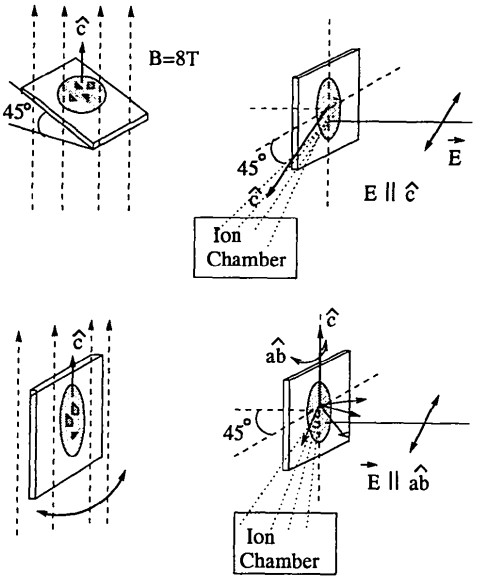

Figure 2
Magnetic alignment geometry used for polarized XAFS measurements. Alignment at 45° from field direction was used for the ĉ-polarized Ni K-edge measurements in fluorescence mode.

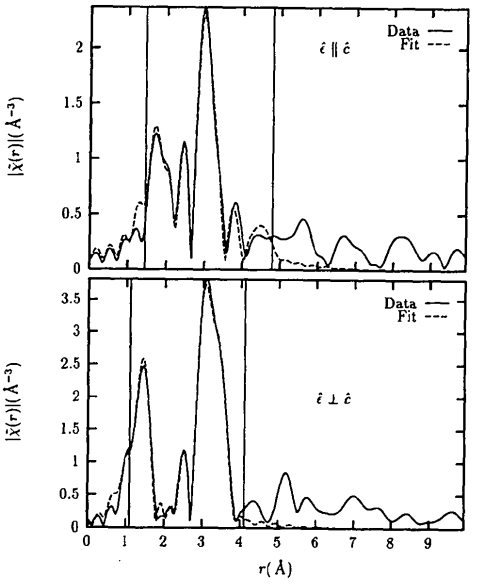

Figure 3
Magnitude of the complex FT of $k^2\chi(k)$ for Ni K-edge in $La_{1.85}Sr_{0.15}Cu_{0.94}Ni_{0.06}O_4$ at T=10K. Transform uses data in $k = [2.5, 12]$ Å^{-1} range; vertical lines indicate fitting regions. Fits used 16 fitting parameters compared to 45 independent points for both polarizations.

Figure 3 shows Ni K-edge fits for both orientations, which include multiple scattering (MS) contributions. Fit results relevant to the discussion here are summarized in Table 1. Whereas planar Ni-O(1) distances remain nearly unchanged (relative to the undoped structure) and only a small expansion in planar Ni-Cu distances is observed (0.016(6) Å), a very large contraction (0.16(1) Å) of the Ni-O(2) apical distances is measured. This contraction propagates along the ĉ-axis, the O(2) motion dragging its neighbor La atom, as seen by the 0.06 Å contraction of the Ni-$La_{\hat{c}}$ distance.

The Ni-O(1)-Cu planar buckling angle α was directly measured by fitting an α-parameterized form of the effective scattering amplitude $F_k(\alpha)$ of these nearly collinear MS paths to $\hat{ab}$-oriented data. The value obtained is in agreement with the average planar buckling angle determined by diffraction (Table 1), again indicating the disorder introduced by Ni in the CuO_2 planes is small compared to the much larger out of plane distortion. No significant differences were found at the Ni K-edge for the different values of y. Temperature dependent (T=10K, 200K) parameterization of the disorder in Ni-O(1), Ni-O(2) and Ni-Cu distances to an Einstein model resulted in Einstein temperatures of $\theta_E = 900 \pm 300$K, $\theta_E = 282 \pm 20$K, $\theta_E = 324 \pm 30$K, respectively. The Ni-O(2) distance expands by 0.006 ± 0.012 Å between T=10K and 200K.

Table 1
Selected fit results at the Ni K-edge. Data corresponds to $y = 0.06$ at T=10K. $S_0^2 = 0.902 \pm 0.067$; the large uncertainty in buckling angle is due to the small variation with α of $F_k(\alpha)$ for small buckling angles near collinearity ($0 \leq \alpha \leq 5°$). Diffraction results are from Radelli *et. al*, 1994.

	XAFS	Diffraction
Ni-O(1)	1.882(8) Å	1.888 Å
Ni-Cu	3.789(6) Å	3.774 Å
Ni-O(2)	2.250(12) Å	2.415 Å
Ni-$La_{\hat{c}}$	4.701(16) Å	4.760 Å
Ni-O(1)-Cu	$\alpha = 2.5 \pm 3°$	$\langle\alpha\rangle = 3.61°$

La K-edge fits are shown in figure 4. The local contraction rate (with Ni) of the c-lattice parameter at T=10K is directly measured as a sum of interatomic distances along ĉ, 2×(La-$Cu_{\hat{c}}$) + (La-$La_{\hat{c}}$), and found to be $dc/dy = -0.0095(25)$[Å/at. %Ni]. This compares well with the corresponding value found in our diffraction analysis at RT, $dy/dc = -0.0080(5)$[Å/at. %Ni] (figure 1). Analysis of Sr K-edge polarized data, however, reveals a *different* response of the Sr atomic environment to Ni doping than that of the La, as exemplified by the Ni-dependence of the La/Sr-$La_{\hat{c}}$ distance along the ĉ axis (figure 5).

4. Discussion

The local contraction of the NiO_6 octahedra indicates that Ni is in its high spin Ni^{+2} ($3d^8$) *non-Jahn-Teller* (JT) state, similar to that found in pure La_2NiO_4 (which has NiO_6 octahedra ~ 0.19 Å shorter along ĉ than CuO_6 octahedra in pure La_2CuO_4). In its high spin state Ni^{+2} has one electron in each of the nearly degenerate $3d_{3z^2-r^2}$ and $3d_{x^2-y^2}$ energy levels and therefore no energy gain is obtained by the octahedral deformation, as degeneracy lifting preserves the center of mass of the e_g manifold. For Cu^{+2} ($3d^9$) in La_2CuO_4 the elongation of CuO_6 octahedra is driven by the energy gain resulting from the *difference* in population of these orbitals.

A low spin Ni^{+2} state or a $3d^7$ configuration would result in elongated NiO_6 octahedra, which is not observed. The disappearance of the JT effect for NiO_6 octahedra should be accompanied by an expansion of its basal plane (the pure nickelate has ~ 0.04 Å larger Ni-O(1) planar distance than the pure cuprate despite Ni^{+2} being a smaller ion than Cu^{+2}). For the case here, however, this expansion is suppressed (table 1) due to the rigidity of the CuO_2 plane embedding the basal plane of the NiO_6 octahedra (highly covalent). The Ni-O(2) "bond" is much softer and therefore the elastic energy cost associated with the observed contraction is small. This is also reflected in the much larger temperature dependence

of the disorder in the Ni-O(2) distances compared to Ni-O(1) (see Einstein temperatures above).

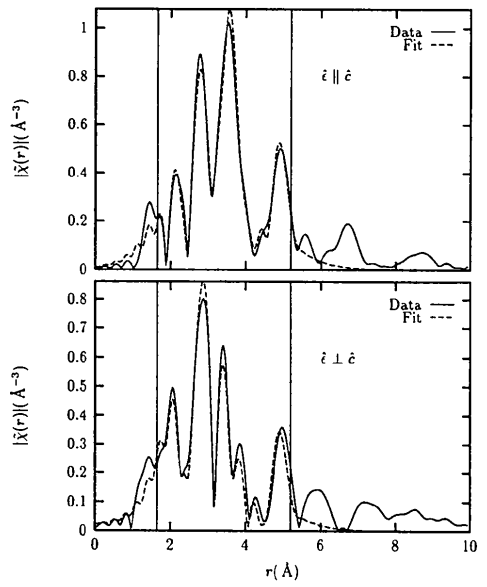

Figure 4
Magnitude of the complex FT of $k^2\chi(k)$ for La K-edge in $La_{1.85}Sr_{0.15}Cu_{0.94}Ni_{0.06}O_4$ at T=10K. Transform uses data in $k = [3, 14]\,\text{Å}^{-1}$ range; vertical lines indicate fitting regions. Fits used 22 fitting parameters compared to 52 independent points for both polarizations.

These findings indicate that Ni does *not* trap hole carriers in $La_{1.85}Sr_{0.15}Cu_{1-y}Ni_yO_4$, as a Ni^{+3} $3d^7$ configuration would have resulted in a JT elongated NiO_6 octahedra. Our polarized XANES measurements at the Ni K-edge are consistent with this conclusion. The localization of hole carriers (metal-insulator transition) observed at about 5 at. %Ni (Cieplak *et. al*, 1992) must therefore occur "away" from the Ni dopant ions. The relevant energies involved in localizing a hole on Ni ($3d^7$ configuration) include (a) the JT energy, i.e., the energy gain resulting from degeneracy lifting of the e_g-manifold versus elastic energy cost of deformation), (b) loss of exchange energy (Hund's energy) associated with destroying the high spin state of Ni.

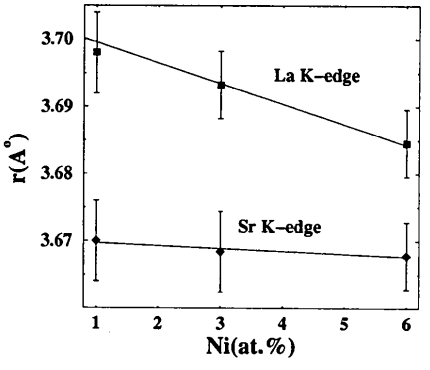

Figure 5
La/Sr-La distance along the $\hat{c}$-axis versus Ni content as obtained from La, Sr K-edge data.

Our finding of a Ni^{+2}, $3d^8$, high spin configuration, as derived from the observed Ni-O(2) contraction (non-JT ion) indicates that the exchange energy (b) dominates which would indicate that Ni "repels" holes to preserve its high spin state. Our results indicate that the spatial distribution of hole carriers is modified by the Ni dopants. Assuming the mobile hole carriers reside in the CuO_2 planes, their wavefunctions will be peaked in between Ni ions. An interesting correlation is that high T_c superconductivity is suppressed at about 3-4 at. % Ni, where the average distance between Ni dopants in the 2D planes is $3.77/\sqrt{y} = 19 - 22$ Å. This is about the size of the in-plane superconducting coherence length, $\zeta_{ab}(0) = 22.7$ Å (Nachumi *et. al*, 1996) for $La_{1.85}Sr_{0.15}CuO_4$. As the smallest region that can sustain superconductivity is of order of ζ_{ab}, it is possible that suppression occurs when holes are constrained to occupy regions smaller than ζ_{ab}.

Our model differs from the "swiss cheese" model of Nachumi *et. al* in that our results predict an inhomogeneous hole charge distribution and increased scattering *in the normal state* (hole poor regions around Ni) leading to spatial inhomogeneity of the superconducting order parameter below T_c. The "swiss cheese" model predicts a uniform normal state charge distribution and the effect of dopants is to remove SC pairs from the superfluid in a $\pi\zeta_{ab}^2$ region around the dopant.

We have previously shown that hole carriers introduced with Sr doping are polaronic in nature and that their wave functions are peaked near the Sr dopant sites (Haskel *et. al*, 1997; Hammel *et. al*, 1998). If Ni "repels" holes a correlation between Ni and Sr atomic positions could be expected. A measurement of the La/Sr relative occupancy ($x/2$) of La/Sr sites near Ni was performed at the Ni K-edge to give $x = 0.048 \pm 0.06$. Whereas this rules out that Sr preferentially occupies sites nearby Ni, the result is consistent with a random distribution of Sr/La ($x/2 = 0.075$) or a tendency of Sr to avoid the Ni immediate environment ($x/2 = 0$). We could not get equivalent information from the Sr K-edge XAFS, as Ni and Cu have nearly the same backscattering amplitudes and therefore are indistinguishable. However, the much smaller response of the local environment of Sr to Ni doping as compared to that of La (figure 5) is suggestive of a tendency of Sr to avoid Ni, as would be expected for doped holes that are peaked "away" from Ni but nearby Sr.

Acknowledgements We thank F. Perez and M. Suenaga for their valuable help and A. Moodenbaugh for the T_c measurements. Research done under auspices of DOE Grant No. DE-FG03-98ER45681.

References

Bernhard, C., Tallon, J. L., Bucci, C., De Renzi, R., Guidi, G., Williams, G. V. M. & Niedermayer, Ch. (1996). *Phys. Rev. Lett.* **77**, 2304–2307.
Bernhard, C., Tallon, J. L., Bucci, C., De Renzi, R., Guidi, G., Williams, G. V. M. & Niedermayer, Ch. (1998). *Phys. Rev. Lett.* **80**, 205–206.
Cieplak, M. Z., Guha, S., Kojima, H., Lindenfeld, P., Xiao, G., Xiao, J. Q. & Chien, C. L. (1992). *Phys. Rev. B* **46**, 5536–5547.
Hammel, P. C., Statt, B. W., Martin, R. L, Chou, F. C., Johnston, D. C.& Cheong, S. W. (1998) *Phys. Rev. B* **57**, R712–R715.
Haskel, D., Stern, E. A., Hinks, D. G., Mitchell, A. W. & Jorgensen, J. D. (1997). *Phys. Rev. B* **56**, R521–R524.
Nachumi, M. E. *et. al* (1996). *Phys. Rev. Lett.* **77**, 5421–5424.
Radaelli, P. G. *et. al. Phys. Rev. B* **49**, 4163–4175.
Stern, E. A., Newville, M., Ravel, B., Yacoby, Y. & Haskel, D. (1995). *Physica B* **208&209**, 117–120.
Suzuki, M. & Hikita, M. (1989). *Jpn. J. App. Phys.* **28**, L1368–L1371.
Zabinsky, S. I., Rehr, J. J., Ankudinov, A., Albers, R. C. & Eller, M. J. (1995). *Phys. Rev. B* **52**, 2995–3009.
Zhitomirsky, M. E. & Walker, M. B. (1998). *Phys. Rev. Lett.* **80**, 5413–5416.

(Received 10 August 1998; accepted 26 January 1999)